Bound-to-bound midinfrared intersubband absorption in carbon-doped GaAs/AlGaAs quantum wells

Oana Malis,[a] Loren N. Pfeiffer, Kenneth W. West, and A. Michael Sergent
Bell Laboratories, Lucent Technologies, 600 Mountain Avenue, Murray Hill, New Jersey 07974

Claire Gmachl
Department of Electrical Engineering and PRISM, Princeton University, Princeton, New Jersey 08544

(Received 3 March 2005; accepted 14 July 2005; published online 25 August 2005)

Bound-to-bound intersubband absorption in the valence band of modulation-doped GaAs quantum wells with digitally alloyed AlGaAs barriers was studied in the midinfrared wavelength range. A high-purity solid carbon source was used for the *p*-type doping. Strong narrow absorption peaks due to heavy-to-heavy hole transitions are observed with out-of-plane polarized light, and weaker broader features with in-plane polarized light. The heavy-to-heavy hole transition energy spans the spectral range between 206 to 126 meV as the quantum well width is increased from 25 to 45 Å. The experimental results are found to be in agreement with calculations of a six-band $\mathbf{k}\cdot\mathbf{p}$ model taking into account the full band structure of the digital alloy. © *2005 American Institute of Physics*.
[DOI: 10.1063/1.2037859]

Intersubband transitions in the conduction band of semiconductor multiple quantum wells (QWs) have been an active field of research over the past twenty years[1] and have led to numerous practical devices, such as quantum-well infrared photodetectors[2] and quantum cascade lasers.[3] Due to the complexities related to the valence band, hole intersubband transitions have not been explored as intensively as their electronic counterparts. Most of the studies of intersubband transitions in the valence band were done in *p*-type Si–SiGe QWs where intersubband absorption, electroluminescence, and photocurrent measurements have been reported.[4–8] Terahertz emission from radiative impurity transitions in the valence band of silicon devices is also currently under investigation.[9] The Si–SiGe material system however presents some significant theoretical and growth challenges associated with the built-in strain of these lattice mismatched materials. The GaAs–AlGaAs system has the advantage of being virtually strain-free and well understood from the material growth point of view. Most of the research in the valence band of this system, however, has been focusing on bound-to-continuum transitions for infrared photodetectors.[10,11] Far-infrared absorption measurements of GaAs/AlGaAs QWs grown on GaAs (311)A substrates have also been reported.[12] We are investigating the properties of bound-to-bound intervalence subband transitions in GaAs QWs with high Al composition barriers for midinfrared emitters. The hole intersubband transitions are particularly interesting because they offer the potential of designing surface-emitting quantum cascade lasers and ultimately vertical-cavity surface-emitting lasers. Moreover, unlike the conduction band, the valence bands of the AlGaAs alloys have their maxima at the respective Γ points throughout the compositional range. The valence-band offset for pure GaAs and AlAs is comparable with the conduction-band offset in the InGaAs/InAlAs lattice matched to InP system (~0.5 eV) and, consequently, hole devices promise to match the midinfrared emission range that is most interesting for practical applications.

This letter presents a study of the midinfrared bound-to-bound intersubband absorption in C-doped GaAs QWs with high Al composition AlGaAs barriers. The GaAs/AlGaAs structures were grown by solid-source molecular-beam epitaxy (MBE) on (100) GaAs substrates. Each sample consists of 50 GaAs QWs with 300Å $Al_{0.57}Ga_{0.43}As$ barriers. In order to reduce the interface roughness and to control the well dimensions with 1% accuracy, the QW widths were chosen to be exact integers of the monolayer spacing: 25.5, 31.13, 36.79, and 45.28 Å corresponding to 9, 11, 13, and 16 monolayers, respectively. The high Al composition AlGaAs is a digital alloy formed by a short-period superlattice of 11.3 Å AlAs and 8.5 Å GaAs. The QWs were modulation doped with carbon using a custom-made solid carbon source. Carbon is preferable to beryllium for *p*-type doping because it has a lower diffusion constant at the MBE growth temperatures. The C source we employed is compatible with very high-purity GaAs material growth, as confirmed by mobility measurements of two-dimensional electron gases. Using Hall measurements, the two-dimensional hole gas for the 31 Å QW sample was estimated to have a density of $1.6\times10^{12}\mathrm{cm}^{-2}$ per QW and mobility of 8000 $\mathrm{cm}^2/\mathrm{V\,s}$ at 5 K.

The midinfrared absorption measurements were done in a multipass waveguide geometry [inset of Fig. 1(a)] at temperatures from 5 K to 300 K using the temperature-controlled cold finger of a helium-flow cryostat. The spectra were taken with a Nicolet Fourier-transform infrared spectrometer equipped with a cooled HgCdTe detector in rapid scan and the signal was averaged over 100 scans.

Figure 1(a) shows the absorption spectra of *s*- (in-plane) and *p*- (out-of-plane) polarized light for the 31 Å QW sample at 17 K. As expected, the *p*-polarized light exhibits strong narrow absorption features due to heavy-hole transitions between the ground and first-excited states. The s-polarized spectrum also exhibits absorption features, but they are smaller in intensity and broader, and are likely due to transitions between the ground heavy-hole state and the first-excited light-hole state. Because the *p*-polarized light has

[a]Electronic mail: malis@lucent.com

 © 2005 American Institute of Physics
Downloaded 31 Aug 2006 to 128.112.35.48. Redistribution subject to AIP license or copyright, see http://apl.aip.org/apl/copyright.jsp

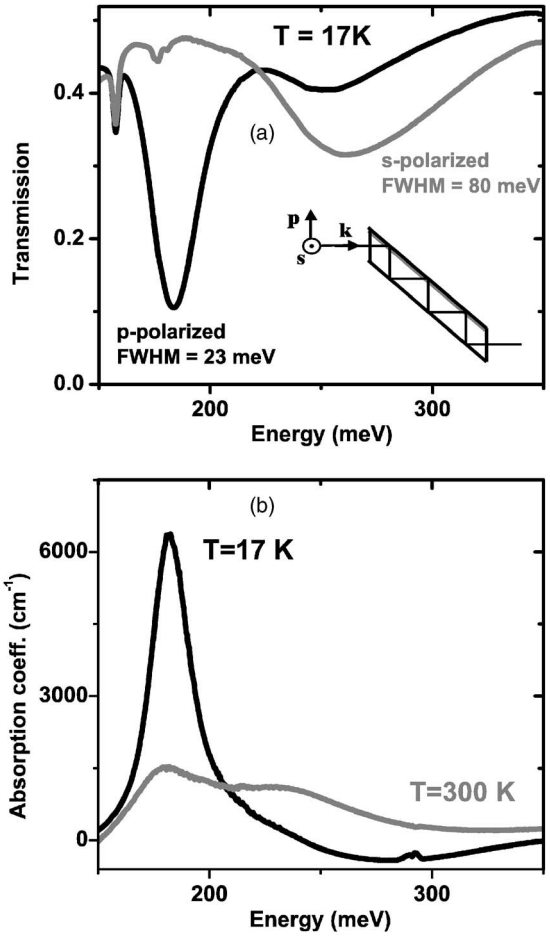

FIG. 1. (a) Midinfrared intersubband transmission spectra of the sample containing 31 Å wide carbon modulation-doped GaAs QWs with digital $Al_{0.57}Ga_{0.43}As$ alloy barriers. The spectra for *p*-polarized (black line) and *s*-polarized (gray line) light are shown for measurements at 17 K. The inset shows the experimental multipass waveguide geometry. (b) Absorption coefficient for the 31 Å QW sample at 17 K (black line) and 300 K (gray line).

both an in-plane and a normal-to-the-plane component, the heavy-to-light transition is also visible in the *p*-polarized spectrum. The heavy-to-heavy hole absorption features can be observed up to room temperature [Fig. 1(b)]. If we ignore the contribution of the heavy-to-light hole transitions, we can define an absorption coefficient α_W in a similar fashion to electron intersubband transitions[13] as $\alpha_W=\ln(T_s/T_p)/L_{\text{int}}$, where T_s and T_p are the transmissions for the *s*- and *p*-polarized light. The transmission was normalized to the signal from a local region of the sample where the QWs were chemically removed. Due to polishing and etching sample nonuniformity, the transmission away from the strong absorption features averages to about 50% instead of 100%. L_{int} is the interaction length given by $L_{\text{int}}=L_{\text{QW}}Nn_p/\cos\theta$, where L_{QW} is the QW width, N is the number of QWs, n_p is the number of passes (11 in our case), and $\theta=45°$ is the incident angle on the QWs. The area under the absorption peak

$$\int \alpha_W L_{\text{int}} dE = \frac{\pi\rho_s N n_p e}{\hbar\varepsilon_0 c n}\frac{\sin^2\theta}{\cos\theta}\Delta E\cdot z_{\text{if}}^2, \tag{1}$$

gives an estimate of the dipole matrix element, z_{if}. ΔE is the transition energy, ρ_s is the hole density, and n is the refractive index. For the heavy-to-heavy hole transition shown in Fig. 1(b), z_{if} is approximately 6 Å, which is about a factor of 3 lower than the typical values for intersubband electron transitions in InGaAs/InAlAs QWs.[13]

TABLE I. Experimental heavy-to-heavy hole transition energies and FWHM of the *p*-polarized absorption spectra for the corresponding QW widths.

QW width (Å)	Energy (meV)	FWHM (meV)
25.50	206	53
31.13	182	23
36.79	160	20
45.28	126	17

The experimental results for the heavy-to-heavy hole transitions are summarized in Table I and Fig. 2(a) for four QW widths. The transition energy decreases from 206 meV to 126 meV when the QW width is increased from 25 to 45 Å. The vertical bars through the peak energy data points indicate the respective full width at half maximum (FWHM) values of the absorption signals. For the 31 Å QW sample, the FWHM is 23 meV, a value that is slightly lower than that reported in *p*-type Si/SiGe QWs (30 meV),[4] but larger than

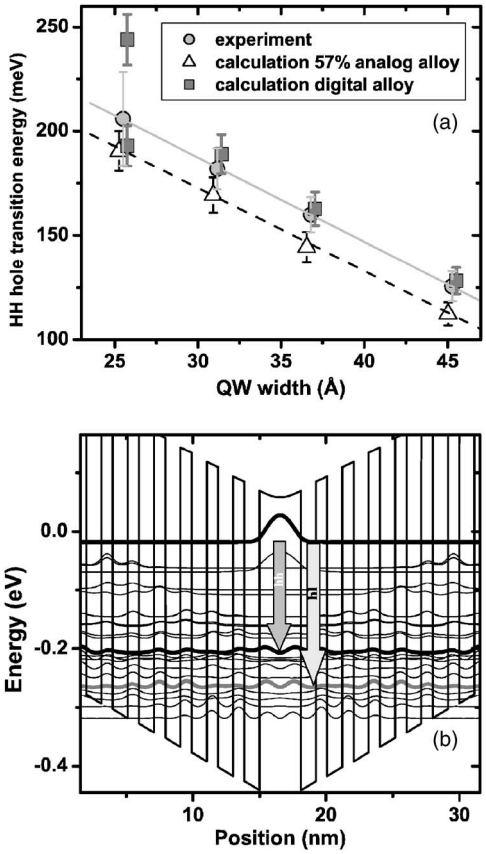

FIG. 2. (a) Comparison of the experimental (circles) heavy-to-heavy hole transition energy for four different QW widths with the calculations of the six-band $k\cdot p$ model assuming the barriers consisting of homogeneous $Al_{0.57}Ga_{0.43}As$ alloy (triangles), and simulating the full band structure of the digital alloy (squares). The calculated points were offset horizontally by ±0.5 Å for clarity. The lines are linear fits through the data to guide the eye. The vertical bars through the experimental data points show the experimental FWHM. For the calculated data, the error bars equal to 10% of the peak transition energies. (b) Full valence-band structure including the detailed structure of the digital alloy barriers for a 31 Å QW *p* doped at the level of $1.6\times10^{12}/\text{cm}^2$. The heavy-to-heavy hole transition is indicated with a dark gray arrow, while the most likely heavy-to-light hole transition is indicated by the light-gray arrow.

Downloaded 31 Aug 2006 to 128.112.35.48. Redistribution subject to AIP license or copyright, see http://apl.aip.org/apl/copyright.jsp

typical values for electron transitions in InGaAs/InAlAs QWs (15 meV).[13]

A theoretical understanding of the hole energy levels corresponding to complex structures is essential for the design of quantum cascade emitters. Therefore, we calculated the QW valence-band diagram in a six-band $\mathbf{k}\cdot\mathbf{p}$ model using the NEXTNANO3 simulation package.[14] The valence-band offset for the pure GaAs and AlAs was taken to be 0.51 eV.[15] The Luttinger parameters in the simulations were taken to be $\gamma_1=8.64$, $\gamma_2=2.44$, $\gamma_3=3.27$, for GaAs (split-off energy of 0.34 eV), and $\gamma_1=5.03$, $\gamma_2=0.8$, $\gamma_3=1.55$, for AlAs (split-off energy of 0.275 eV). The calculations were done self-consistently to include the direct Coulomb effect of the charge redistribution due to the modulation doping. No attempt was made at this time to estimate the many-body effects, such as exchange-correlation, depolarization, or exciton shift, but the sum of these effects is expected to be less than 10% in our narrow QWs.[1] Figure 2(a) shows the results for the heavy-to-heavy hole transition energies assuming the barriers are made of a homogeneous $Al_{0.57}Ga_{0.43}As$ alloy. The model reproduces the overall data dependence on the well width, but it consistently underestimates the transition energies. We believe this effect is mainly due to the digital alloying technique used for the growth of the AlGaAs barriers. Because pure AlAs layers surround the GaAs QW, the digital alloy effectively increases the valence-band offset seen by the holes. We performed transition energy calculations taking into account the full band structure of the QW and digital alloy. Figure 2(b) shows the band structure and energy levels for a 31 Å QW with digital alloy barriers doped at the level of $1.6\times10^{12}/cm^2$. The comparison of the experimental and digital alloy simulation results can be seen in Fig. 2(a). This model agrees very well with the experimental data for the three wider wells. For the 25 Å wide well the calculations predict a manifold of closely spaced mixed transitions that are not visible in the experimental data. The two lowest-lying transition energies indicated in Fig. 2(a) are in rough agreement with the measurement. One may conclude then that the model overestimates the penetration of the superlattice miniband of the digital barrier into the QW, and thus overestimates optical transition probabilities to its states. This effect is visible even for the 31 Å wide well [Fig. 2(b)], but in this case the transition identified with the dark-gray arrow is dominant. The in-plane band dispersion was found to have a small effect on the transition energies (less than 10 meV) at the hole densities corresponding to the experimental measurements.

In contrast with the *p*-polarized absorption peaks, a satisfactory identification of the transitions corresponding to the in-plane absorption features is considerably more challenging. For the 31 Å QW, the transition energy of 260 meV is likely due to a heavy-to-light hole transition. In the homogeneous AlGaAs alloy model, the transition energy of the *s*-polarized peak is high enough to point to a bound-to-continuum type of transition resonantly enhanced by the remnants of the first excited light-hole state.[11] The digital alloy calculations produce several possible transitions in this spectral range. The most likely candidate (shown as the thick gray line) gives a transition energy that is 13 meV lower than the experimental value. More sophisticated simulations including many-body effects may be necessary to accurately predict the in-plane polarized absorption spectra.

In conclusion, the intersubband absorption of *p*-type doped GaAs QWs with digitally alloyed AlGaAs barriers was measured in the midinfrared. The structures were grown by MBE using a C-doping technique that is compatible with very high-purity GaAs. The spectra exhibit strong absorption peaks in the *p*-polarized light due to bound-to-bound heavy-to-heavy hole transitions. For a QW 25 to 45 Å wide, the absorption peak covers a broad midinfrared range (206–126 meV, i.e. $\sim 6-10$ μm wavelength), that is promising for application in quantum cascade emitters. Six-band $\mathbf{k}\cdot\mathbf{p}$ calculations of the heavy-to-heavy hole transition energies considering the full band structure of the digitally alloyed barriers are in very good agreement with the experimental results for wider wells. The model is less accurate in predicting the out-of-plane absorption for the narrowest wells, as well as the in-plane absorption features. The discrepancies between the experiment and calculations may be due to many-body effects, such as exchange correlations, depolarization, and excitonic effects.[1,11,16,17] The slightly larger than typical simulation parameters used in our calculations may be partially compensating for some of these effects. More experimental and theoretical investigations are needed to unfold the various contributions of these effects to the measured transition energies. For all practical purposes, however, the model is accurate enough to be adequate for band structure calculations of complex multiple QW structures, such as the quantum cascade lasers.

The authors would like to acknowledge fruitful discussions with F. Szmulowicz of the Air Force Research Laboratory, and J. Meyer of the Naval Research Laboratory.

[1] M. Helm, Semicond. Semimetals **62**, 1 (2000) and references therein.
[2] H. C. Liu, Semicond. Semimetals **62**, 129 (2000) and references therein.
[3] C. Gmachl, F. Capasso, D. L. Sivco, and A. Y. Cho, Rep. Prog. Phys. **64**, 1533 (2001) and references therein.
[4] L. Diehl, H. Sigg, G. Dehlinger, D. Grützmacher, E. Müller, U. Gennser, I. Sagnes, T. Fromherz, Y. Campidelli, O. Kermarrec, D. Bensahel, and J. Faist, Appl. Phys. Lett. **80**, 3274 (2002).
[5] G. Dehlinger, L. Diehl, U. Gennser, H. Sigg, J. Faist, K. Ensslin, D. Grützmacher, and E. Müller, Science **290**, 2277 (2000).
[6] I. Bormann, K. Brunner, S. Hackenbuchner, G. Zandler, G. Abstreiter, S. Schmult, and W. Wegscheider, Appl. Phys. Lett. **80**, 2260 (2002).
[7] L. Diehl, S. Mentee, E. Müller, D. Grützmacher, H. Sigg, U. Gennser, I. Sagnes, Y. Campidelli, O. Kermarrec, D. Bensahel, and J. Faist, Appl. Phys. Lett. **81**, 4700 (2002).
[8] I. Bormann, K. Brunner, S. Hackenbuchner, G. Abstreiter, S. Schmult, and W. Wegscheider, Appl. Phys. Lett. **83**, 5371 (2003).
[9] P.-C. Lv, R. T. Troeger, S. Kim, S. K. Ray, K. W. Goossen, J. Kolodzey, I. N. Yassievich, M. A. Odnoblyudov, and M. S. Kagan, Appl. Phys. Lett. **85**, 3660 (2004).
[10] B. F. Levine, S. D. Gunapala, J. M. Kuo, S. S. Pei, and S. Hui, Appl. Phys. Lett. **59**, 1864 (1991).
[11] F. Szmulowicz and G. J. Brown, Phys. Rev. B **51**, 13203 (1995); F. Szmulowicz, A. Shen, H. C. Liu, G. J. Brown, Z. R. Wasilewski, and M. Buchanan, *ibid.* **61**, 13798 (2000); H. C. Liu, T. Oogarah, E. Dupond, Z. R. Wasilewski, M. Byloos, M. Buchanan, F. Szmulowicz, J. Ehret, and G. J. Brown, Electron. Lett. **38**, 909 (2002).
[12] B. E. Cole, J. M. Chamberlain, M. Henini, V. Nakov, and G. Gobsch, J. Appl. Phys. **80**, 6058 (1996).
[13] C. Sirtori, F. Capasso, J. Faist, and S. Scandolo, Phys. Rev. B **50**, 8663 (1994).
[14] ⟨http://www.nextnano.de⟩ or ⟨http://www.wsi.tu-muenchen.de/nextnano3/⟩
[15] S.-H. Wei and A. Zunger, Appl. Phys. Lett. **72**, 2011 (1998).
[16] K. M. S. V. Bandara, D. D. Coon, O. Byungsung, Y. F. Lin, and M. H. Francombe, Appl. Phys. Lett. **53**, 1931 (1988).
[17] S. K. Chun, D. S. Pan, and K. L. Wang, Phys. Rev. B **47**, 15638 (1993).

Downloaded 31 Aug 2006 to 128.112.35.48. Redistribution subject to AIP license or copyright, see http://apl.aip.org/apl/copyright.jsp